Journal of
Materials Chemistry A

Accepted Manuscript

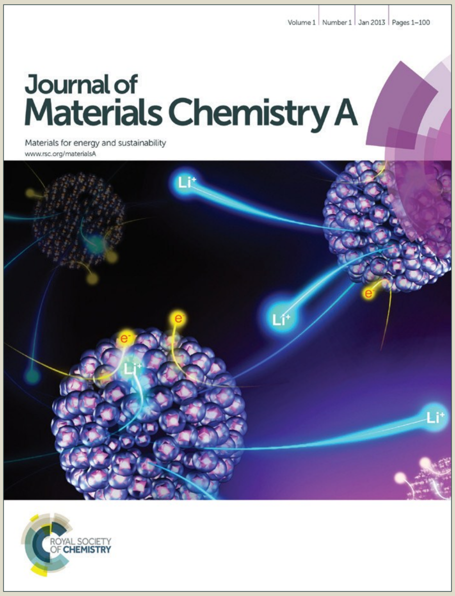

ROYAL SOCIETY
OF CHEMISTRY

www.rsc.org/materialsA

Journal Name

ARTICLE

Received 00th January 20xx,
Accepted 00th January 20xx

DOI: 10.1039/x0xx00000x

www.rsc.org/

Fabrication of Ultrathin Solid Electrolyte Membranes of β-Li_3PS_4 Nanoflakes by Evaporation-Induced Self-Assembly for All-Solid-State Batteries

Hui Wang,[1,*] Zachary D. Hood,[1,2] Younan Xia,[2,3,4] Chengdu Liang[1,*]

All-solid-state lithium batteries are attractive candidates for next-generation energy storage devices because of their anticipated high energy-density and intrinsic safety. Owing to their excellent ionic conductivity and stability with metallic lithium anode, nanostructured lithium thiophosphate solid electrolytes such as β-Li_3PS_4 have found use in the fabrication of all-solid lithium batteries for large-scale energy storage systems. However, current methods for preparing air-sensitive solid electrolyte membranes of lithium thiophosphates can only generate thick membranes that compromise the battery's gravimetric/volumetric energy-density and thus its rate performance. To overcome this limitation, the solid electrolyte's thickness needs to be effectively decreased to achieve ideal energy-density and enhanced rate performance. Herein, we show that the evaporation-induced self-assembly (EISA) technique produces ultrathin membranes of lithium thiophosphate solid electrolyte with controllable thicknesses between 8-50 µm while maintaining the high ionic conductivity of β-Li_3PS_4 and stability with metallic lithium anode up to 5 V. It is clearly demonstrated that the facile EISA approach allows for the preparation of ultrathin lithium thiophosphate solid electrolyte membranes for all-solid-state batteries.

Introduction

Rechargeable batteries employing metallic Li anode attract strong research interest because of their high theoretical capacity (3,860 mAh g^{-1}) and the lowest electrochemical potential.[1,2] Batteries that employ organic liquid electrolytes suffer from Li dendrite growth, which results in serious problems such as short-circuiting, poor cycling performance, and unavoidable safety hazards. Switching to solid electrolytes provides a viable solution to construct safer and longer-lasting batteries. The solid electrolyte's mechanical integrity can prevent the penetration of Li dendrites while its thermal stability eliminates crucial safety concerns associated with conventional liquid electrolytes.[3,4]

An all-solid-state lithium battery consists of three indispensable components: a Li metal anode, a cathode, and a solid electrolyte. The solid electrolyte is crucial in a solid-state battery since it plays the dual roles of transporting Li ions and separating electrodes. As a result, the solid electrolyte directly determines the energy-density of a battery as well as the battery's rate performance and cyclability. Sulfide-based materials are finding widespread use as solid electrolytes because of their potential higher ionic conductivities than oxides at room temperature.[5,6,7] Higher ionic conductivities allow the large-scale energy storage systems to perform more efficiently. Nanostructured lithium thiophosphate solid electrolytes such as β-Li_3PS_4 have excellent ionic conductivity and stability with metallic lithium anode, which render these electrolytes as promising candidates for large-scale applications. Though β-Li_3PS_4 has a plethora of ideal properties for solid-state battery applications, it is still hard to process this material as thin membranes.

Thick solid electrolyte pellets largely deteriorate the performance in solid-state batteries and pose a huge challenge for the commercialization of such batteries. Multiple difficulties are presented in synthesizing thin solid electrolyte membranes for all-solid-state batteries, primarily due to the lack of efficient and inexpensive solid electrolyte processing

---

[1] *Center for Nanophase Materials Sciences, Oak Ridge National Laboratory, Oak Ridge, TN 37831, USA. E-mail: wangh1@ornl.gov; cd_liang@hotmail.com*
[2] *School of Chemistry and Biochemistry, Georgia Institute of Technology, Atlanta, Georgia, 30332, USA*
[3] *Wallace H. Coulter Department of Biomedical Engineering, Georgia Institute of Technology and Emory University, Atlanta, GA 30332, USA*
[4] *School of Chemical and Biomolecular Engineering, Georgia Institute of Technology, Atlanta, GA 30332, USA*

methods. Traditional cold/warm pressing approaches are easy to operate, but usually result in pellets with hundreds of micrometers in thickness.[5,8,9] Other thin film techniques—such as pulsed laser deposition (PLD) and radio frequency (RF) magnetron sputtering—are appropriate for depositing amorphous solid electrolyte films of oxide-based materials but may not be cost-effective for air- or moisture- sensitive sulfide-based solid electrolytes.[9,10,11,12] Therefore, the exploration of convenient, low-cost techniques is urgent for producing thin sulfide-based solid electrolyte membranes.

Herein, we demonstrate that evaporation-induced self-assembly (EISA) can be utilized to produce additive-free, solid electrolyte membranes from β-Li_3PS_4 nanoflakes with controllable thicknesses between 8-50 µm. This technique has a number of advantages, including ease of operation, low cost, and high reproducibility.[13,14] As such, EISA has been recognized as one of the most efficient and facile routes to prepare ordered nano/micro structures.[15,16,17] To our knowledge, this work represents the first attempt to apply EISA to the preparation of ultrathin solid electrolyte membranes for all-solid-state batteries.

Experimental Section

Synthesis of β-Li_3PS_4 Nanoflakes: Li_2S (Alfa Aesar, 99.9%) and P_2S_5 (Sigma-Aldrich, 99%) with a stoichiometry of 3 to 1 were mixed in anhydrous acetonitrile (ACN, Sigma-Aldrich, >99.8%) at room temperature. A white precipitate was observed after the mixture was stirred for 48 h. After vacuum filtration, the obtained precipitate was treated at 80 °C to remove excess solvent, yielding $Li_3PS_4 \cdot 2ACN$. Further heat treatment at 200 °C produced a pure phase of β-Li_3PS_4. Considering lithium thiophosphate's sensitivity to air, all the experimental procedures were carried out in an argon-filled glove box.

EISA membrane preparation: Pure β-Li_3PS_4 powder was dispersed in ACN solvent to form a fine suspension. A thin β-Li_3PS_4 membrane was obtained by dip-coating Ni foil in the suspension followed by step-wise heat treatment at 80°C and 200°C under vacuum to remove ACN complexed with Li_3PS_4. The membrane thickness was tuned by varying the suspension concentrations (0.16 M, 0.25 M, and 0.4 M). In addition, thicker membranes were also obtained by repeating the dip-coating process. The thicker β-Li_3PS_4 membranes (>30 µm) could be peeled from the Ni substrate to form freestanding films, however, a full piece (1/2 inch) of the substrate-free membrane is still difficult to obtain. Therefore, a 50 µm substrate-free β-Li_3PS_4 membrane was pressed with β-Li_3PS_4 nanoflakes for electrochemical evaluation on the stability between metallic lithium anode and the thin solid electrolyte membranes.

Structural and electrochemical characterizations: Crystallographic phase identification was conducted using a PANalytical X'pert Pro Powder Diffractometer with a Copper Kα line. Samples for XRD analysis were prepared in a glovebox on zero background slides sealed with Kapton® films. SEM images of β-Li_3PS_4 thin films from EISA (on Ni substrate without pressing) were obtained using a field-emission scanning electron microscope (FE-SEM, Zeiss Merlin) equipped with a specially designed stage for handling air-sensitive samples. Ionic conductivity and Arrhenius activation energy measurements were completed using β-Li_3PS_4 membranes (diameter 12.5 mm, thickness ≈30 µm) pressed with carbon-coated aluminum foil as the blocking electrodes. For the Arrhenius activation energy measurements, the temperature was controlled from 25 °C to 100 °C in a temperature-controlled chamber (Maccor, ±0.5 °C). Electrochemical impedance spectroscopy (EIS) measurements were taken using a 1260 Solartron Frequency Response Analyzer between 1 MHz and 0.1 Hz at amplitude of 100 mV. Swagelok® cells were used to complete all cyclic voltammetry (CV) and cycling performance measurements. For the CV measurements, thin β-Li_3PS_4 membranes (diameter is 12.5 mm, thickness ≈50 µm) were cold-pressed at 200 MPa and Li foil and Pt foil were carefully attached on each side. The Li/β-Li_3PS_4/Pt cell was carried out at a rate of 100 mVs^{-1} between −0.2 and 5 V vs. Li/Li^+ at room temperature using a Bio-Logic VSP multi-channel potentiostat. For the symmetric cells, a β-Li_3PS_4 membrane (12.5 mm in diameter, ~50 µm in thickness) was pressed and then two Li foils (7 mg) were carefully attached to both sides, respectively. The Li/β-Li_3PS_4/Li symmetric cell was cycled on a battery test system (Bio-Logic) with different current densities (0.20, 0.50, 0.75 mA cm^{-2}) at room temperature. A control experiment was completed with a thick β-Li_3PS_4 pellet (diameter is 12.5 mm, thickness ≈500 µm) for comparison.

Results and Discussion

A schematic illustration of the EISA method using Li_3PS_4 nanoflakes to form ultrathin membranes is shown in Figure 1. Compared with spheres and rods, flakes have a larger aspect ratio α (α is defined as D/t, where D is the literal diameter and t is the thickness). Because of the large aspect ratio, flakes tend to stack "face-to-face" in rows with their faces parallel and edges perpendicular to the substrate in a process under the influence of capillary forces.[18] Once the faces of the nanoflakes stack in a "face-to-face" manner, the edges of the flakes will fuse together in an "edge-to-edge" fashion. Therefore, the nanoflakes dispersed in a solvent are expected to easily form thin, dense membranes upon solvent evaporation.

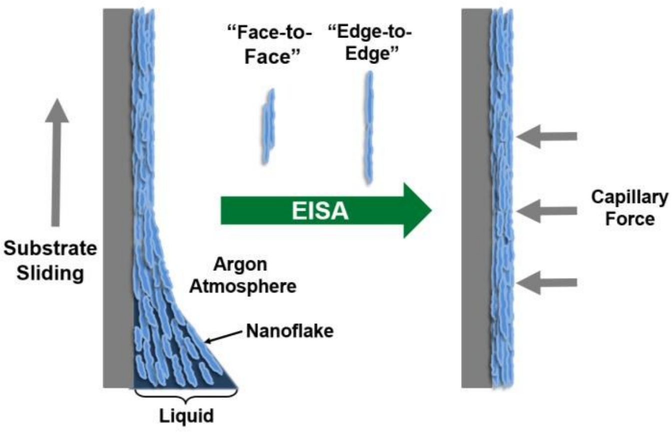

Figure 1. Schematic of evaporation induced self-assembly (EISA) of β-Li_3PS_4 nanoflakes under argon. The basic principle of EISA is that solvent evaporation causes individual components to associate into an ordered structure driven by the capillary force.

β-Li_3PS_4 nanoflakes were synthesized using a wet chemistry method. Lithium sulfide (Li_2S) reacts with phosphorus pentasulfide (P_2S_5) in acetonitrile (ACN), resulting in the formation of a white precipitate in the ACN solution. The precipitate is a complex with a stoichiometric composition of $Li_3PS_4{\cdot}2ACN$, and the removal of ACN at 200 °C produces pure β-Li_3PS_4. This process is shown in Equation (1):

$$3\,Li_2S + P_2S_5 \xrightarrow{\text{excess ACN}} 2\,Li_3PS_4{\cdot}2ACN \xrightarrow{200\,°C} 2\,\beta\text{-}Li_3PS_4 + 4\,ACN_{(g)}\uparrow \quad (1)$$

Figure 2a shows an SEM image of the as-synthesized β-Li_3PS_4 powder, which is composed of nanoflakes. The nanoflakes are characterized by two sharply different length scales: the lateral size varies from 1 to 2 μm whereas the thickness is around 80 nm for all nanoflakes (inset in Figure 2a). The β-Li_3PS_4 nanoflakes display a structure distinct from that of β-Li_3PS_4 synthesized through tetrahydrofuran (THF), which produces larger nanoporous particles with an average size of ~8 μm (Figure 2b), as discussed in our previous report.[19] The difference in particle size and morphology can be attributed to the difference in solvent-solid interaction during the wet chemistry synthesis process. Compared with the large chunks, fine flakes should form thin membranes more readily. Furthermore, the large aspect ratio (α = > 12) for nanoflakes enlarges the face-to-face interaction areas, which is beneficial to the formation of ultrathin membranes.

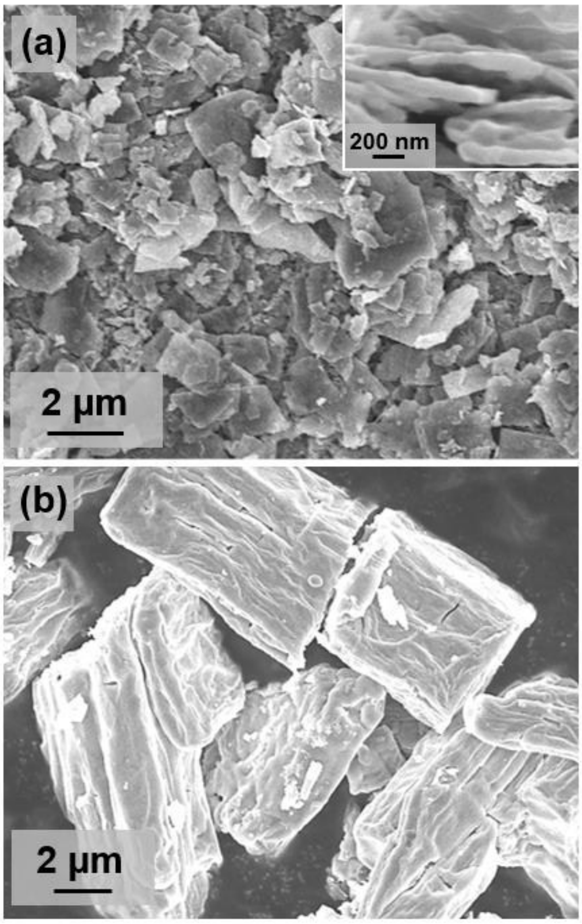

Figure 2. Characterization of nanostructured Li_3PS_4. SEM image of (a) β-Li_3PS_4 from ACN (nanoflakes with average lateral diameter of 2 μm and thickness of 80 nm) and (b) β-Li_3PS_4 from THF (nanoporous particles with an average particle size of 8 μm).

X-ray diffraction (XRD) patterns confirmed Li_3PS_4 nanoflakes as the β phase (Figure 3a). The characteristic diffraction peaks at 2θ = 16.6°, 17.5°, 27.0°, 28.4°, 29.3° and 30.2° indicate solvent removal from the $Li_3PS_4{\cdot}2ACN$ complex and the production of pure β phase of Li_3PS_4. Unlike the bulk γ phase, β-Li_3PS_4 has a higher conductivity because of its large interstitials characteristic of its crystalline structure and the decreased Li site occupancy.[19,20,21] β-Li_3PS_4 nanoflakes exhibits a high ionic conductivity of 1.2

$\times10^{-4}$ S cm^{-1} at room temperature and an Arrhenius activation energy of 0.36 eV (Figure 3d). The Li ionic conductivity for β-Li_3PS_4 nanoflakes is slightly lower than the value for nanoporous β-Li_3PS_4 synthesized from THF[19] (1.6$\times10^{-4}$ S cm^{-1}), which might be related to the decreased surface conduction in thin films produced with β-Li_3PS_4 nanoflakes. The comparison indicates that the morphology does not adversely compromise the high Li^+ conductivity characteristic of the solid electrolyte.

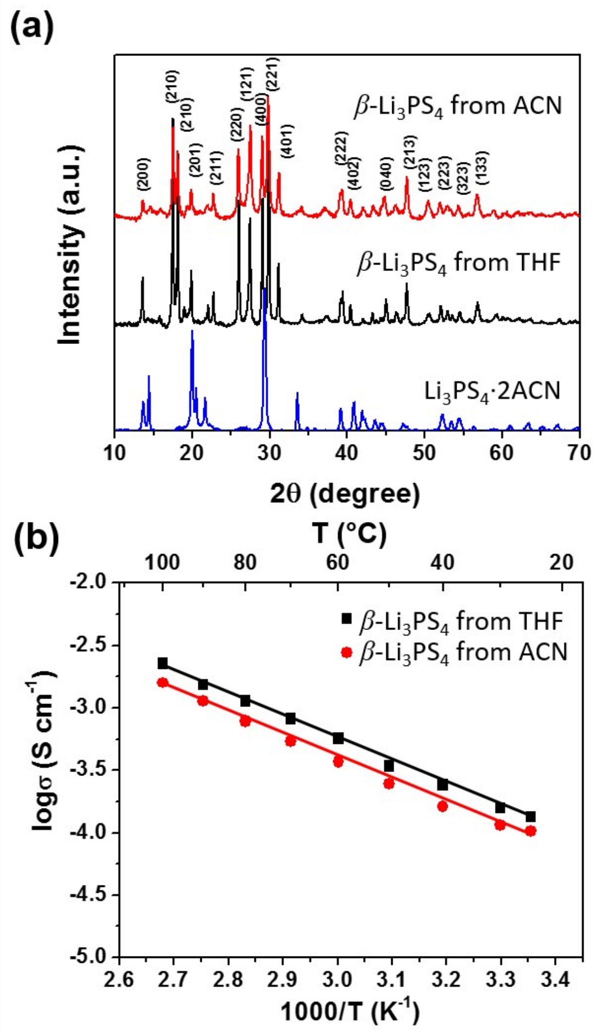

Figure 3. (a) XRD patterns of β-Li_3PS_4 from ACN, β-Li_3PS_4 from THF, and the $Li_3PS_4{\cdot}2ACN$ complex; (b) Arrhenius plots of β-Li_3PS_4 from ACN and β-Li_3PS_4 from THF.

For β-Li_3PS_4 nanoflakes, EISA is considered to be a desirable technique to produce thin membranes for two main reasons: (1) β-Li_3PS_4 flakes are able to form a fine suspension in ACN solvent; and (2) the nanoflakes will favor a "face-to-face" arrangement since this arrangement generates strong attractive forces between each individual flake. The EISA coating process starts with dip-coating a homogeneous suspension of β-Li_3PS_4 on a nickel (Ni) substrate. During the drying process, the evaporation of the solvent increases the concentration of solute within the depositing film, resulting in β-Li_3PS_4 nanoflakes aligned in a parallel "face-to-face" pattern, which is driven by capillary forces. Further solvent evaporation causes a self-assembly of ordered nanoflakes to propagate through the membrane. Thus, the combination of "edge-to-edge" arrangement at each layer and "face-to-face" arrangement between layers produces highly ordered and dense β-Li_3PS_4 membranes. Figure 4 presents scanning electron microscopy (SEM) images of β-Li_3PS_4 nanoflakes membranes on a Ni substrate prepared through the EISA method. Figure 4a shows an SEM image of the top view of the membrane, where nanoflakes connect with one another in an "edge-to-edge" arrangement to form a smooth, homogeneous surface. The edges of five pieces can be clearly observed at higher magnification, as indicated by the blue lines in Figure 4a. In addition, the small pores on the surface confirm the removal of solvent during heat treatment to produce pure β-Li_3PS_4. The cross-sectional SEM image (Figure 4b) reveals a dense β-Li_3PS_4 membrane that has a thickness of ~8 µm. The EISA prepared β-Li_3PS_4 film has good contact with the Ni substrate. No obvious pores or cracks were observed, indicating the good quality of the solid electrolyte membrane.

The membranes prepared through the EISA method were significantly thinner than solid electrolyte membranes prepared through traditional hot/cold pressing methods.[22,23,24,25] Furthermore, the thickness of the β-Li_3PS_4 membranes formed by EISA is controllable under different processing parameters. In this work, we tuned the concentration of β-Li_3PS_4 in ACN while employing the same EISA technique to gain thickness control for the sulfide-based membranes. A 0.16 M β-Li_3PS_4 suspension produced an 8 µm solid membrane, whereas increasing the suspension concentration leads to thicker β-Li_3PS_4 membranes (~12 µm and ~18 µm, Figure S1). Interestingly, EISA allows for the preparation of additive-free β-Li_3PS_4 membranes without a substrate (Figure S2), which is ideal for battery assembly since additives can affect the membrane's performance. These results clearly prove that EISA is an efficient approach to produce ultrathin solid β-Li_3PS_4 membranes that dramatically reduce the solid electrolyte thickness by two orders of magnitude when compared to hot/cold pressing methods.

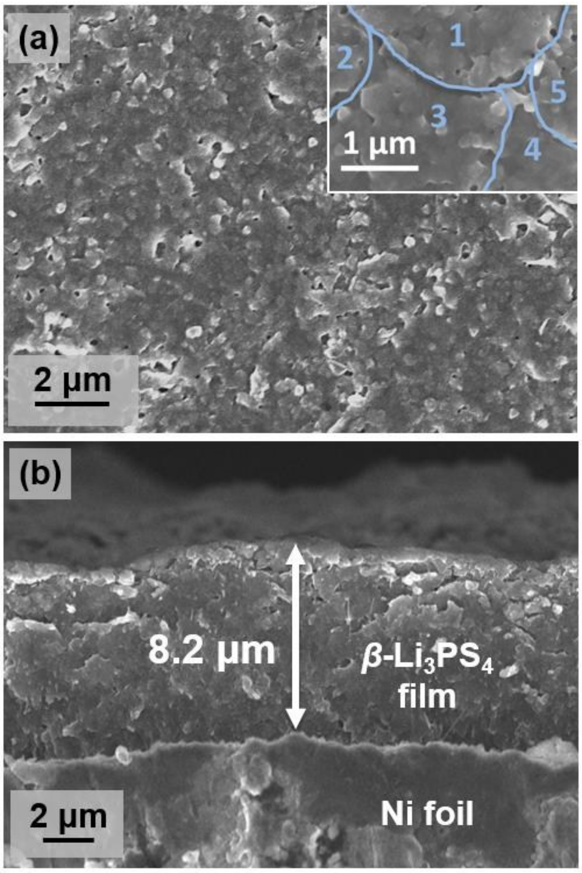

Figure 4. SEM images of ultrathin solid electrolyte membranes of β-Li$_3$PS$_4$ nanoflakes produced by EISA: (a) top view (inset is at a higher magnification, where the blue lines represent the region where the edges of nanoflakes join); (b) cross-sectional image of a β-Li$_3$PS$_4$ membrane (thickness = 8.2 µm) on a Ni substrate.

The compatibility of thin solid electrolyte membranes with metallic lithium anode is crucial for constructing high-performance all-solid-state lithium batteries. Therefore, it is important to evaluate the stability and cyclability of thin β-Li$_3$PS$_4$ membranes with metallic lithium anode. Given that ACN is employed as the solvent for the EISA process, Li foil is not an appropriate substrate since possible side reactions can occur on the lithium metal surface. To investigate the compatibility, we prepared a free-standing membrane of β-Li$_3$PS$_4$ nanoflakes with a reasonable thickness of 50 µm.

Figure 5a shows the cyclic voltammogram (CV) of a Li/β-Li$_3$PS$_4$/Pt cell from −0.2 to 5.0 V (vs. Li$^+$/Li). A pair of reversible oxidation and reduction peaks were observed at around 0 V (vs. Li$^+$/Li). The cathode current below 0 V corresponds to Li deposition, and the anode current results from lithium dissolution. No other side reactions appeared on the CV, as we only observed peaks corresponding to lithium deposition and stripping. These results indicate that membranes of β-Li$_3$PS$_4$ nanoflakes have good stability with metallic lithium anode over a broad electrochemical window. This observation is unlike other highly ion-conducting solid electrolytes (e.g., Li$_{10}$GeP$_2$S$_{12}$) from earlier reports,[5,26] which showed strong interfacial reactions with metallic lithium. Furthermore, it was also confirmed that the nanoflake morphology for β-Li$_3$PS$_4$ improves the processing properties while maintaining its electrochemical stability with metallic Li anode.

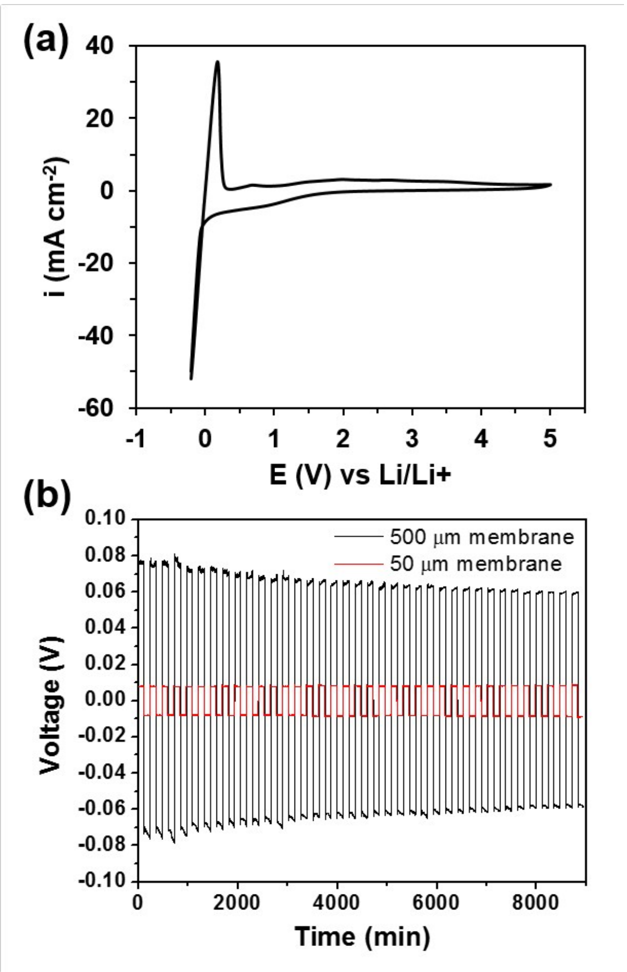

Figure 5. Electrochemical stability and cycling ability of the thin solid electrolyte membranes of β-Li$_3$PS$_4$ nanoflakes with metallic lithium electrodes: (a) CV of a Li/β-Li$_3$PS$_4$/Pt cell, with metallic Li and platinum as the reference/counter and working electrodes, respectively. (b) Cycling data of two symmetric cells (Li/β-Li$_3$PS$_4$/Li) with β-Li$_3$PS$_4$ solid electrolyte membranes measuring 50 µm and 500 µm.

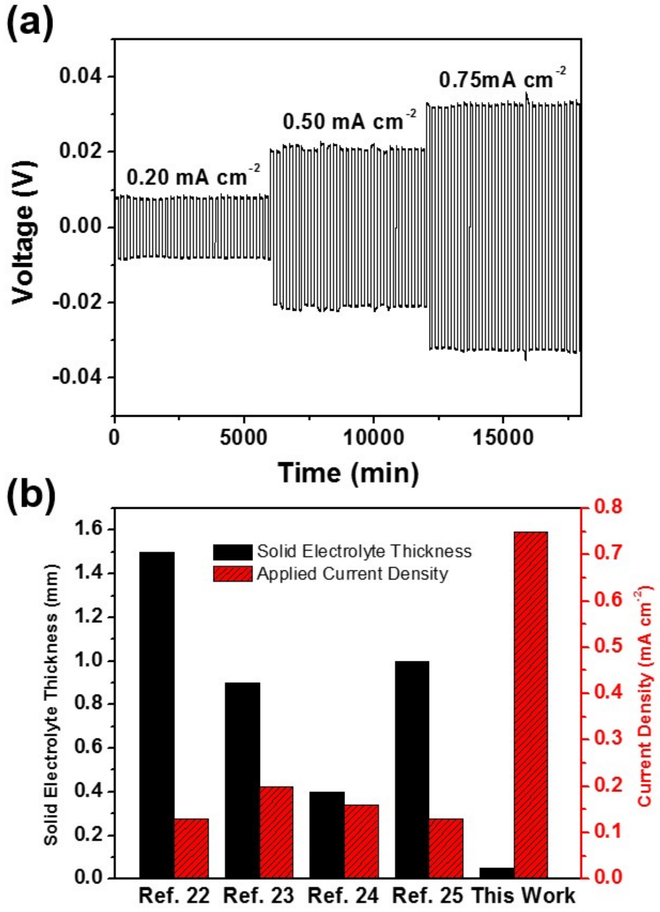

Figure 6. (a) Cycling data of a symmetric cell under different current densities (0.2, 0.5, and 0.75 mA cm^{-2}) with a 50-µm thick membrane fabricated from β-Li_3PS_4 nanoflakes; (b) a comparison of the sulfide-based solid electrolyte thicknesses and applied current densities, indicating that decreasing the solid electrolyte membrane allows for larger current densities.

To further demonstrate the cyclability and long-term compatibility of the thin β-Li_3PS_4 membranes with Li metal, a symmetric Li/β-Li_3PS_4/Li cell was assembled with a 50 µm solid electrolyte membrane. As a basis for comparison, a control experiment was carried out by fabricating of a symmetric Li/β-Li_3PS_4/Li cell with a thicker solid electrolyte membrane (500 µm). Figure 5b presents the data of two symmetric cells cycled under the same current density of 0.2 mA cm^{-2}. A minimal polarization of 8 mV was observed at room temperature, which is almost 10 times lower than that of the cell with a thicker solid electrolyte membrane (75 mV). Such a small polarization allows for a larger current applied to the cell, and as a result, the rate performance is greatly improved.[27] As shown in Figure 6a, when the current density increased to 0.50 and 0.75 mA cm^{-2}, the Li/β-Li_3PS_4/Li cell with a 50 µm membrane presented a linear relationship, as the voltage increased to 20 and 32 mV, respectively. This correlation indicates that there is negligible interfacial resistance between the lithium electrode and the solid electrolyte, further confirming that the thin membrane is completely compatible with metallic lithium anode. Previous studies reported that the β-Li_3PS_4/Li interface doesn't show an appreciable interfacial reaction after multiple cycles.[19,28] It is worth noting that the current density for the ultrathin membranes reported in this work is as high as 0.75mA cm^{-2}, much greater than the values reported in literatures (Figure 6b). [22,23,24,25] A high current density allows for a rapid and efficient transport of lithium ions through the solid electrolyte membrane. As such, all-solid-state batteries employing ultrathin solid electrolyte membranes will have an overall better rate performance and require an overall shorter charging time between cycles.

Conclusions

In summary, we have demonstrated the use of EISA as a simple and versatile technique to fabricate thin membranes of a sulfide-based solid electrolyte. We first developed a wet-chemistry method to prepare β-Li_3PS_4 nanoflakes with high ionic conductivity and then used EISA to assemble them into dense, thin membranes with thicknesses controllable in the range of 8-50 µm. The as-obtained membranes showed excellent electrochemical stability with metallic lithium anode. The EISA approach was found to be both facile and inexpensive when applied to the fabrication of sulfide-based membranes for all-solid-state lithium batteries. With some further development, this technique will have an important impact on the fabrication of high energy-dense and low-cost all-solid-state batteries.

Acknowledgements

This research was conducted at the Center for Nanophase Materials Sciences in Oak Ridge National Laboratory, which is a U.S. Department of Energy (DOE) Office of Science User Facility. CL was supported by U.S. DOE, Office of Basic Energy Sciences (BES), Materials Sciences and Engineering Division, U.S. DOE. ZDH gratefully acknowledges a Graduate Research Fellowship award from the National Science Foundation (DGE-1148903) and the Georgia Tech-ORNL Fellowship.

References

1. D. P. Lv, Y. Y. Shao, T. Lozano, W. D. Bennett, G. L. Graff, B. Polzin, J. G. Zhang, M. H. Engelhard, N. T. Saenz, W. A. Henderson, P. Bhattacharya, J. Liu, J. Xiao, *Adv Energy Mater* **2015**, *5*.
2. W. Xu, J. L. Wang, F. Ding, X. L. Chen, E. Nasybutin, Y. H. Zhang, J. G. Zhang, *Energ Environ Sci* **2014**, *7*, 513-537.
3. R. Murugan, V. Thangadurai, W. Weppner, *Angew Chem Int Edit* **2007**, *46*, 7778-7781.
4. Z. Y. Tu, Y. Kambe, Y. Y. Lu, L. A. Archer, *Adv Energy Mater* **2014**, *4*.
5. N. Kamaya, K. Homma, Y. Yamakawa, M. Hirayama, R. Kanno, M. Yonemura, T. Kamiyama, Y. Kato, S. Hama, K. Kawamoto, A. Mitsui, *Nat Mater* **2011**, *10*, 682-686.
6. E. Rangasamy, Z. C. Liu, M. Gobet, K. Pilar, G. Sahu, W. Zhou, H. Wu, S. Greenbaum, C. D. Liang, *J Am Chem Soc* **2015**, *137*, 1384-1387.
7. J. A. Brant, D. M. Massi, N. A. W. Holzwarth, J. H. MacNeil, A. P. Douvalis, T. Bakas, S. W. Martin, M. D. Gross, J. A. Aitken, *Chem Mater* **2015**, *27*, 189-196.
8. F. Mizuno, A. Hayashi, K. Tadanaga, M. Tatsumisago, *Adv Mater* **2005**, *17*, 918-+.
9. Y. J. Nam, S. J. Cho, D. Y. Oh, J. M. Lim, S. Y. Kim, J. H. Song, Y. G. Lee, S. Y. Lee, Y. S. Jung, *Nano Lett* **2015**, *15*, 3317-3323.
10. E. Quartarone, P. Mustarelli, *Chem Soc Rev* **2011**, *40*, 2525-2540.
11. A. Sakuda, A. Hayashi, T. Ohtomo, S. Hama, M. Tatsumisago, *J Power Source*, **2011**, *196*, 6735-6741.
12. Y. Ito, A. Sakuda, T. Ohtomo, A. Hayashi, M. Tatsumisago, *J Ceram Soc Jpn*, **2014**, *122*, 341-345.
13. C. J. Brinker, Y. F. Lu, A. Sellinger, H. Y. Fan, *Adv Mater* **1999**, *11*, 579-+.
14. J. X. Huang, F. Kim, A. R. Tao, S. Connor, P. D. Yang, *Nat Mater* **2005**, *4*, 896-900.
15. C. T. Black, C. B. Murray, R. L. Sandstrom, S. H. Sun, *Science* **2000**, *290*, 1131-1134.
16. A. Pucci, M. G. Willinger, F. Liu, X. B. Zeng, V. Rebuttini, G. Clavel, X. Bai, G. Ungar, N. Pinna, *Acs Nano* **2012**, *6*, 4382-4391.
17. A. Tao, P. Sinsermsuksakul, P. Yang, *Nat Nanotechnol* **2007**, *2*, 435-440.
18. N. R. Jana, *Angew Chem Int Edit* **2004**, *43*, 1536-1540.
19. Z. C. Liu, W. J. Fu, E. A. Payzant, X. Yu, Z. L. Wu, N. J. Dudney, J. Kiggans, K. L. Hong, A. J. Rondinone, C. D. Liang, *J Am Chem Soc* **2013**, *135*, 975-978.
20. K. Homma, M. Yonemura, T. Kobayashi, M. Nagao, M. Hirayama, R. Kanno, *Solid State Ionics*, **2011**, *182*, 53-58.
21. M. Tachez, J. P. Malugani, R. Mercier, G. Robert, *Solid State Ionics* **1984**, *14*, 181-185.
22. S. Teragawa, K. Aso, K. Tadanaga, A. Hayashi, M. Tatsumisago, *J Mater Chem A* **2014**, *2*, 5095-5099.
23. T. Yamada, S. Ito, R. Omoda, T. Watanabe, Y. Aihara, M. Agostini, U. Ulissi, J. Hassoun, B. Scrosati, *J Electrochem Soc* **2015**, *162*, A646-A651.
24. T. Ohtomo, A. Hayashi, M. Tatsumisago, K. Kawamoto, *J Solid State Electr* **2013**, *17*, 2551-2557.
25. A. Hayashi, H. Muramatsu, T. Ohtomo, S. Hama, M. Tatsumisago, *J Mater Chem A* **2013**, *1*, 6320-6326.
26. G. Sahu, Z. Lin, J. C. Li, Z. C. Liu, N. Dudney, C. D. Liang, *Energ Environ Sci* **2014**, *7*, 1053-1058.
27. M. Park, X. C. Zhang, M. D. Chung, G. B. Less, A. M. Sastry, *J Power Sources* **2010**, *195*, 7904-7929.
28. Z.D.Hood, H. Wang, Y.C. Li, A.S. Pandian, M. P. Paranthaman, and C.D. Liang. "The “filler effect”: A study of solid oxide fillers with β-Li 3 PS 4 for lithium conducting electrolytes." *Solid State Ionics* 283 (2015): 75-80.

Fabrication of Ultrathin Solid Electrolyte Membranes of β-Li_3PS_4 Nanoflakes by Evaporation-Induced Self-Assembly for All-Solid-State Batteries

Hui Wang,[1,*] Zachary D. Hood,[1,2] Younan Xia,[2,3,4] Chengdu Liang[1,*]

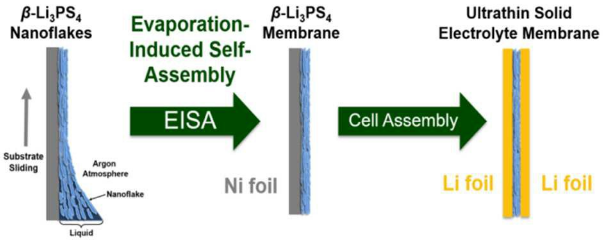

Evaporation-induced self-assembly produces ultrathin solid electrolyte membranes of β-Li_3PS_4 while maintaining its high ionic conductivity and stability with metallic Li.